Bull. Chem. Soc. Jpn. Vol. 84, No. 11, 1251–1260 (2011)

Tailoring the Surface Chemistry of Activated Carbon by Nitric Acid: Study Using Response Surface Method

Amirhossein Houshmand, Wan Mohd Ashri Wan Daud,* and Mohammad Saleh Shafeeyan

Department of Chemical Engineering, Faculty of Engineering, University of Malaya, 50603 Kuala Lumpur, Malaysia

Received May 18, 2011; E-mail: ashri@um.edu.my

Tailoring the surface chemistry of adsorbents, especially activated carbons, make them suitable to specific applications. Many times oxidation is the first step and greatly affects the next steps of tailoring. We modified the surface chemistry of a microporous activated carbon (AC) by nitric acid solutions at different conditions of acid concentration, time, and oxidation temperature. The oxidized AC samples were inspected with the aid of physical adsorption–desorption of nitrogen at 77 °C and temperature-programmed desorption (TPD). It was shown that oxidation by nitric acid lowers surface area of the studied AC even at mild severity. Moreover, different instrumental analysis pointed out creation of a considerable amount of oxygen-containing functional groups, especially acidic ones on the surface. Central composite design (CCD) was applied to evaluate the individual and interactive effects of oxidation parameters and to provide a compromise between the amount of oxygen groups and BET surface area as two of studied responses. The significant factors and interactions on each response were recognized by Analysis of Variance (ANOVA). A linear model and a two factor interaction (2FI) model were developed to correlate the oxidation conditions to BET surface area and the amount of oxygen surface groups. In addition, optimized oxidation conditions were established.

These days, activated carbons (ACs) are suitably used in the role of adsorbent, catalyst, or catalyst support due to their great surface area and obvious chemical activity. Textural characteristics and surface chemistry of AC has been reviewed by the authors.[1]

The ability to tailor the surface chemistry of ACs gives them an amplified value to be used in a wide range of applications. ACs may gain some functional groups on preparation. Types and density of these functional groups depend on precursor and preparation procedure. With coal, petroleum, coke, wood, fruit stone, coconut shell, and so on as the precursor, ACs have mainly oxygen-containing functional groups, whereas precursors such as nitrogen-enriched polymers,[2] urea–formaldehyde and melamine–formaldehyde[3] result in carbon adsorbents with nitrogen surface groups.

AC surface can be modified by various functional groups, molecules, and polymers. These modifiers may improve carbon characteristics for a particular application. Moreover, functional groups may be used for further modification, because in some cases AC surface initially suffers from the lack of chemically reactive functional groups appropriate for a desired modification.

Oxidation is a common method to create oxygen-containing functional groups of different types such as carboxyl and its derivatives (that is lactones and carboxylic anhydrides), phenolics and carbonyls on the surface of AC. The results published in the literature demonstrate that oxidation is regarded as one of the most important procedures for target or preliminary modification of AC surface.

In some cases, oxidation is used as target modification. For example, acidic groups created by oxidation favor catalytic wet air oxidation of aniline.[4] Moreover, the acidic groups improve metal ion or metallic species adsorption[5–8] from solution by ion-exchange and complex formation mechanism. In the latter, acidic groups also assist dispersion of catalyst[9–12] on the AC surface. The acidic surface groups also enhance adsorption of some organic compounds such as sulfur compounds (e.g., in fuel desulfurization),[13–15] acetaldehyde (under some conditions, depending on degree of oxidation and acetaldehyde concentration),[16] and aqueous ammonia.[17]

On the other hand, anchoring different organic molecules on AC surface through some oxygen-containing groups (as coupling agent) point out the application of oxidation as a preliminary modification of AC. The authors have reviewed modification of AC with amino groups for CO_2 capture.[18] As mentioned in this review paper, different amine-containing compound can attach on the surface of AC via the specified oxygen groups as coupling agents. These organic molecules include, but are not limited to, diamines,[19–21] aminosilanes,[19,22,23] 5,11,17,23-tetra(*tert*-butyl)-25,27-bis(2-aminobutoxy)calix[4]arene (a calix[4]arene derivative)[24] and transition-metal complexes such as nickel Schiff base complexes.[25] Furthermore, acidic groups influence the type and degree of amination at low temperatures (200–400 °C) so amide and amine groups are produced as major nitrogen functionalities.[26–29]

Oxidation may be classified as dry and wet processes.[30] Dry oxidation is performed by using an oxidizing gas such as steam, oxygen, carbon dioxide, or ozone usually at elevated temperatures (>700 °C), whereas wet oxidation is carried out by liquid oxidizing agents at mild temperatures (20–100 °C). Although there are various liquid oxidants, the most studied are nitric acid, sulphuric acid, hydrogen peroxide, and ammonium persulfate. It was reported that oxidation with nitric acid can be

Published on the web November 9, 2011; doi:10.1246/bcsj.20110145

controlled by concentration and temperature.[31] For a specified oxidant, parameters including oxidant concentration, time, and temperature of oxidation determine the severity of oxidation.

Generally, the effects of oxidation of AC on its texture and chemistry depend on the inherent nature of oxidant, oxidation conditions, and severity, and origin and history of preparation and activation of the carbon. Therefore, it is rational that different, and sometimes opposite, results are reported for oxidation. For example, some researchers reported that wet oxidation decreases surface area of AC,[7,16,32–35] whereas some reports suggest a constant or increased surface area.[16,28,35–38] Researches show that AC activated at low temperature, is more seriously affected by oxidation than AC activated at high temperature,[39] because the former is subjected to destruction by oxidation.[28]

The mentioned parameters also affect the nature and amount of created oxygen groups. Of the oxidizing agents that can be used for AC oxidation, nitric acid is the most conventional one, because oxidizing specifications can be controlled by concentration and temperature.[1] Nitric acid treatment is a good way to increase carboxylic and phenolic groups in higher order as reported by researchers.[40,41]

Palm shell as a biomass solid waste is a suitable source for preparation of AC in countries such as Malaysia.[42,43] In the present work, modification of a commercial palm shell activated carbon by nitric acid was studied. A trial version of Design Expert software 8.0 was used to apply central composite design (CCD) to design the oxidation experiments in which three oxidation parameters including oxidant concentration, time of oxidation, and process temperature are considered the main variables to modify AC. Changes in AC in terms of its textural characteristics and surface chemistry were discussed qualitatively and quantitatively. Of the measured characteristics of AC, BET surface area and a defined index of the amount of oxygen surface groups were adopted as the responses for response surface methodology (RSM) study. Two appropriate models were developed for these two responses.

Experimental

Materials. The AC was supplied by Bravogreen Sdn Bhd, Malaysia. After sieving to the size range of 500–850 micron (μm), AC was washed with distilled water to remove fines. Then it was dried in the oven at 110 °C overnight and kept in closed bottles for experiments (referred to as A1). Reagent-grade nitric acid was bought from Fisher Scientific, Malaysia.

Oxidation Methods. To design the experiments, CCD was used (see following section). For each of the designed oxidation experiments, a five-gram sample of A1 was reacted with 100 mL of the required acidic solution in a jacketed (double-walled) glassy reactor. The reactor was equipped with a condenser to keep the volume of solution constant during oxidation. A constant-temperature water stream provided by a water bath was circulating in the jacket of the reactor to keep the reactor contents at the desired temperature. A polymer-coated magnetic stirrer was used to mix the content of the reactor. The oxidized AC samples were washed extensively with distilled water until pH of 5 reached. The products were then dried in an oven overnight and kept in closed bottles for analysis.

Characterization Methods. **Textural Characteristics:** Physical adsorption–desorption of nitrogen at 77 K, carried out by ThermoFinnigan Sorptomatic 1990 Series analyzer was used to measure textural characteristics of the samples. Before taking adsorption data, the samples were outgassed using the degas port of the same apparatus at 120 °C and a residual pressure of 300 μmHg for 16 h (overnight).

BET surface area (S_{BET}) was obtained based on adsorption data in the relative pressure (P/P_0) range of 0.01 to 0.3. Total pore volume (V_t) was determined at $P/P_0 = 0.995$. Moreover, linear regression was applied to the adsorption data in the low relative pressure range (less than $P_0/P = 0.3$) using DR equation in the following form[27] to calculate the line intercept and then micropore volume (referred to here as $V_{\mathrm{mic(DR)}}$).

$$\log W = \log V_{\mathrm{mic(DR)}} + M \times \log^2\left(\frac{P_0}{P}\right) \tag{1}$$

Where M is related to adsorption energy, E

$$M = -2.303 \times \left(\frac{RT}{E}\right)^2 \tag{2}$$

Surface Chemistry: Temperature-programmed desorption (TPD), a well-known technique to study chemistry of activated carbon surface, was exploited by using Chemisorb 2720 (Micromeritics). The instrument works on the principle of difference in thermoconductivity of carrier gas and the desorbed gases. Of the possible carrier gases, helium was selected because it has the highest difference of thermoconductivity with the expected evolved gases (CO and CO_2). A 25 mL min^{-1} flow rate of He and a temperature ramp rate of 5 °C min^{-1} from ambient temperature up to 1050 °C was applied to all samples. Thermoconductivity detector (TCD) signal from the apparatus was monitored and recorded to study the evolved gases. Each peak of the TPD spectrum resulted from decomposition of a specified surface group and its evolution as CO and/or CO_2. The area below each peak corresponds to the density of the related group. In other words, the density of oxygen surface groups is proportional to the area below TPD curve. Therefore, we calculated the area below each TPD curve and considered it as an index of oxygen surface groups available on the sample. This term is called Oxygen Index in this paper and used as a response for RSM study.

Experimental Design and Data Analysis. CCD as the most popular RSM design was applied in this study. Experimental design technique and especially RSM is appropriate for analyzing the effects of the parameters, understanding the interactions of the parameters and also for optimizing the desired responses.[44–46]

The total number of experiments in a process optimization conducted by RSM is lower than the method called one factor at a time.[44] For an independent factor number of k, CCD is composed of $(2k + 2k + n_c)$ runs or experiments:[45] $2k$ is the number of the core factorial runs, which are at all possible combination of all the factors at their low and high levels (coded as -1 and $+1$). $2k$ is the number of axial or star runs. Each star point occurs at α time of high/low level of one factor while the other factors are at their center values. In other words, star points are located at $(\pm\alpha, 0, 0)$, $(0, \pm\alpha, 0)$, and $(0, 0, \pm\alpha)$.

Table 1. Design Matrix and Obtained Results

Run (Sample) No.	Factor A: Acid concentration		Factor B: Temperature		Factor C: Time		Response $Y1$: BET surface area /$m^2\,g^{-1}$	Response $Y2$: Oxygen Index —
	Actual /$mol\,L^{-1}$	Coded	Actual /°C	Coded	Actual /h	Coded		
1	2	−1	25	−1	2	−1	786.3	87.3
2	8	1	25	−1	2	−1	722.5	99.1
3	2	−1	70	1	2	−1	727.6	96.3
4	8	1	70	1	2	−1	670.1	115.2
5	2	−1	25	−1	8	1	767.1	90.5
6	8	1	25	−1	8	1	716.9	107.0
7	2	−1	70	1	8	1	703.1	109.5
8	8	1	70	1	8	1	639.0	130.1
9	3.5	−0.5	47.5	0	5	0	746.5	99.0
10	6.5	0.5	47.5	0	5	0	710.0	107.5
11	5	0	36.25	−0.5	5	0	732.0	99.3
12	5	0	58.75	0.5	5	0	695.9	109.5
13	5	0	47.5	0	3.5	−0.5	731.7	101.1
14	5	0	47.5	0	6.5	0.5	718.5	106.5
15	5	0	47.5	0	5	0	723.7	102.9
16	5	0	47.5	0	5	0	732.9	102.8
17	5	0	47.5	0	5	0	730.9	103.6
18	5	0	47.5	0	5	0	706.0	105.2
19	5	0	47.5	0	5	0	726.6	103.5
20	5	0	47.5	0	5	0	721.6	104.0

The value of α, which is the distance between the center and axial points, depends on the number of factors and is calculated as $(2^k)^{0.25}$.[45] However, Design-Expert gives the option of selecting the value of α by the user. Finally, n_c is the number of runs replicated at center point of all factors. The center point runs are used to calculate the experimental error.[46]

In this study, three factors of oxidation time, oxidation temperature, and oxidant concentration were considered as independent variables, while oxidation setup and all the inputs imposed by the setup were deemed as fixed. BET surface area and index of oxygen surface groups are the two responses selected for RSM study, referred to as $Y1$ and $Y2$, respectively. With six replications at center point and the value of α fixed at 0.5 for our purpose, a five-level CCD consisting of 20 runs is designed and performed. Design matrix with coded and actual values of parameters and the obtained responses is shown in Table 1. High and low levels of the parameters were selected based on preliminary experimental work performed by the available setup.

The second-order (quadratic) polynomial equation, whose simplified forms are used here to model the desired responses, is in general form of:

$$Y = \beta_0 + \sum_{i=1}^{n} \beta_i x_i + \sum_{i=1}^{n} \beta_{ii} x_i^2 + \sum_{i=1}^{n}\sum_{j=1}^{n} \beta_{ij} x_i x_j + e \quad (3)$$

Where Y is the modeled response, x represents the independent variables; β is the regression coefficient, and e is error. β_0 is constant value. $\beta_i x_i$ and $\beta_{ii} x_i^2$ represent linear terms (first-order effects of variables) and quadratic terms (second-order effects of the variables), respectively, and $\beta_{ij} x_i x_j$ is a two factor interaction term. This equation does not take the interaction between three factors or more into account. Equation 3 may be simplified to linear equation by setting β_{ii} and β_{ij} as 0. In addition, a two factor interaction (2FI) model can be derived from eq 3 by setting β_{ii} as 0.

For optimizing the process, first of all, the requirements for the responses and factors were established. Then, a set of operating conditions was found at which all responses are optimized or in their accepted ranges.

Results and Discussion

Development of Regression Models. Table 2 displays fit summary of the models evaluated by the software of Design-Expert to find models that can describe the desired responses (BET surface area and Oxygen Index) efficiently and satisfactorily.

As it is evident from the table, the software suggests a linear model for $Y1$ and a two factor interaction (2FI) model for $Y2$. As criteria for model suggestion by the software, the highest order polynomial model where the additional terms are significant and the model is not aliased is proposed. The coded models for response $Y1$ and for response $Y2$ are as follows:

$$Y1 = +720.45 - 29.86A - 31.89B - 10.24C \quad (4)$$

And

$$Y2 = 104.00 + 8.48A + 8.51B + 4.93C + 1.4AB + 0.80AC + 2.13BC \quad (5)$$

Where A, B, and C are coded parameters, refer to acid concentration, temperature, and time, respectively. The models in terms of actual variables are as follows:

$$\mathit{BET\ surface\ area} = +854.59794 - 9.95490 \times \mathit{Acid\ Concentration} - 1.41725 \times \mathit{Temperature} - 3.41176 \times \mathit{Time} \quad (6)$$

And

Table 2. Evaluated Models for Responses of BET Surface Area (*Y*1) and Oxygen Index (*Y*2) by Design Expert Software

Evaluated models	Sequential *p*-value	Lack of Fit *p*-value	Std. Dev.	*R*-squared	Adjusted *R*-squared	Predicted *R*-squared	
Response *Y*1: BET surface area							
Linear	**<0.0001**	**0.7515**	**8.3392**	**0.9390**	**0.9275**	**0.9028**	**Suggested**
2FI	0.6367	0.6890	8.6858	0.9462	0.9214	0.7573	
Quadratic	0.1113	0.9520	7.4310	0.9697	0.9424	0.8287	
Cubic	0.8769	0.9153	8.7911	0.9746	0.9194	−0.4743	Aliased
Response *Y*2: Oxygen Index							
Linear	<0.0001	0.0189	2.0439	0.9554	0.9471	0.8833	
2FI	**<0.0001**	**0.5290**	**0.8734**	**0.9934**	**0.9903**	**0.9621**	**Suggested**
Quadratic	0.2390	0.6314	0.8141	0.9956	0.9916	0.9561	
Cubic	0.4451	0.8588	0.8021	0.9974	0.9918	0.5887	Aliased

Table 3. ANOVA Results of the Linear Model for BET Surface Area Response

Source	Sum of squares	df	Mean square	*F*-value	*p*-value (Prob > *F*)	
Model	17114.93	3	5704.98	82.04	<0.0001	significant
A: Acid concentration	7581.16	1	7581.16	109.01	<0.0001	
B: Temperature	8643.31	1	8643.31	124.29	<0.0001	
C: Time	890.47	1	890.47	12.80	0.0025	
Residual	1112.68	16	69.54			
Lack of Fit	650.13	11	59.10	0.64	0.7515	not significant
Pure Error	462.55	5	92.51			
Cor Total	18227.61	19				

Table 4. ANOVA Results of the Two Factor Interaction (2FI) Model for Oxygen Index Response

Source	Sum of squares	df	Mean square	*F*-value	*p*-value (Prob > *F*)	
Model	1489.17	6	248.20	325.35	<0.0001	significant
A: Acid concentration	610.73	1	610.73	800.58	<0.0001	
B: Temperature	614.98	1	614.98	806.15	<0.0001	
C: Time	206.54	1	206.54	270.75	<0.0001	
AB	15.68	1	15.68	20.55	0.0006	
AC	5.12	1	5.12	6.71	0.0224	
BC	36.13	1	36.13	47.35	<0.0001	
Residual	9.92	13	0.76			
Lack of Fit	6.08	8	0.76	0.99	0.5290	not significant
Pure Error	3.83	5	0.77			
Cor Total	1499.09	19				

$$\begin{aligned}\mathit{Oxygen\ Index} &= +78.32000 + 1.39586 \times \mathit{Acid\ Concentration}\\ &\quad + 0.11693 \times \mathit{Temperature} - 0.29668 \times \mathit{Time}\\ &\quad + 0.020741 \times \mathit{Acid\ Concentration} \times \mathit{Temperature}\\ &\quad + 0.088889 \times \mathit{Acid\ Concentration} \times \mathit{Time}\\ &\quad + 0.031481 \times \mathit{Temperature} \times \mathit{Time} \qquad (7)\end{aligned}$$

The terms positively added to the model have synergistic effects, whereas negative terms have antagonistic effect.[46] From design matrix (Table 1), BET surface area is found to be in the range of 639.0 to 786.3 while Oxygen Index is changed from a minimum of 87.3 to a maximum of 130.1. The adopted models can be used for prediction of the responses in the design space.

Analysis of variance (ANOVA) is further performed here to discuss the suggested models and their terms. ANOVA results are shown in Tables 3 and 4 for BET surface area and Oxygen Index, respectively.

Model suggestion should be integrated with the adequacy check of the model to make sure that the tolerable fit is achieved. Three statistical tests are essential to evaluate the suggested model(s) as follows:[45] *R*-Squared (R^2) test, the test of significance of the model, factors and their interactions, and the test of lack of fit (LOF).

Correlation coefficient or R^2 is a statistical measurement indicating the goodness of fit of the data by the model. R^2 of 1 suggests a perfect fit by the model and the closer of R^2 to 1 is a sign that the values predicted by the model are closer to the response experimental values. As it can be seen from Table 2, R^2 of *Y*1 is 0.9390. This value of R^2 expresses that 93.9% of the total variation of BET surface is ascribed to the considered variables

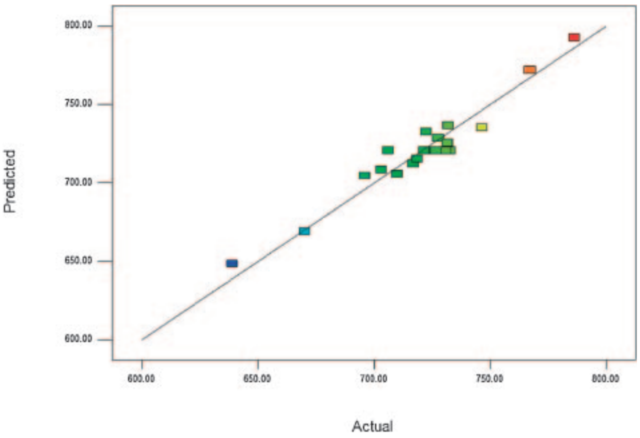

Figure 1. The plot of predicted vs. experimental BET surface area.

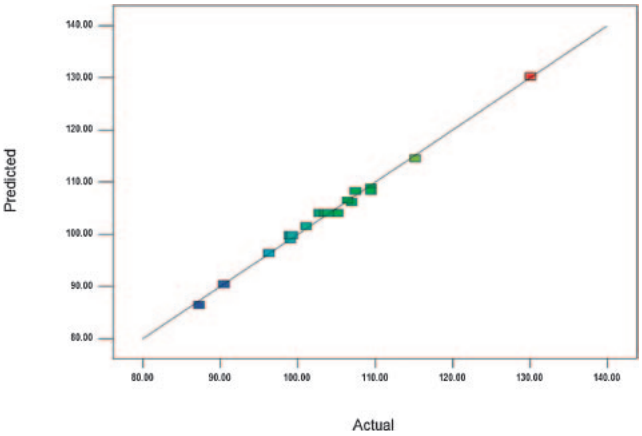

Figure 2. The plot of predicted vs. experimental Oxygen Index.

(i.e., not due to noise or unattended variables) and is justified by the adopted model.[44,46] This states a satisfactory fit. In the same manner, 95.54% of total variation of Oxygen Index response ($R^2 = 0.9554$) is due to the studied variables. This R^2 indicates the predicted response agrees quite well with the experimental response. In other words, the suggested models can correlate the responses to the independent variables successfully.

The plots of the predicted versus actual values have been displayed in Figures 1 and 2 for $Y1$ and $Y2$, respectively. These diagnostic plots graphically show that the predicted values are pretty close to the experimental ones, as already described by statistical term of R^2.

Other than R^2, the models can be discussed in terms of adjusted R^2 and predicted R^2. By adding new terms to a model, the value of R^2 goes up, whereas the adjusted R^2 does not always increase.[45] Usually, adjusted R^2 is compared to predicted R^2. The agreement between adjusted R^2 and predicted R^2 is said to be reasonable if they are within 0.2 of each other.[45] Table 2 shows that the values of the predicted R^2 of 0.9028 and 0.9621 for $Y1$ and $Y2$, respectively are in reasonable agreement with the adjusted R^2 of 0.9275 and 0.9903.

p-value and F-value (Fisher variation ratio) determine if the suggested models are significant or not. A probability value (p-value) of less than 0.05 means significance of the model at the 95% confidence level. The model F-value of 82.4 and p-value of less than 0.0001 for BET surface area response (Table 3) indicate that the suggested model is significant. Moreover, according to Table 4, F-value and p-value for Oxygen Index response are 325.35 and <0.0001, respectively, pointing out to a significant model.

F-value and p-value also determine which factors need to be included in the model or excluded from it. So the terms with a p-value less than 0.05 must be included in the model. It is concluded from Table 3 that all the considered factors for experimental design, i.e., acid concentration, temperature, and time are significant in the model suggested for BET surface area at 95% confidence interval due to their p-value of less than 0.0001. As well, the linear model suggests that there is no significant interaction between the factors that can be included in the model of $Y1$. However, regarding response $Y2$, two factor interactions are significant as well as individual factors. Table 4 shows that p-value of all terms of the Oxygen Index model is less than 0.05 and so all are considered significant.

If a model is strongly affected by the design points, it may predict other points not so well. Except those design points used for the model coefficients, extra design points are used for the test of lack of fit. The variation between the model prediction and the extra points is compared with the pure error to test the lack of fit. By the lack of fit test, one can verify if systematic or random error is responsible for deviation of expected values from the measured ones. Significant lack-of-fit means that the variation of the replicates about their mean values is less than the variation of the design points about their predicted values. The result of this test should be insignificant indicating there is no significant lack of fit. A small F-value and high p-value (greater than 0.1) are good in this test. From Tables 3 and 4, lack of fit p-value for $Y1$ and $Y2$ are 0.7515 and 0.5290 (F-values are 0.64 and 0.99), respectively. These values imply that lack of fit is insignificant for both suggested models.

As well F-value and p-value, adequate precision (AP) and coefficient of variation (CV) are other indicators that can be used for evaluating significance of the model.[44] Adequate precision which is considered as a signal to noise ratio, is a measure of the range in predicted response relative to its associated error. A value greater than 4 is desired. Our ratios of 38.606 (for BET surface area response) and 84.811 (for Oxygen Index response) indicate adequate signals. So the models can be used to navigate the design space. The coefficient of variation is a measure of residual variation of the data relative to the size of the mean. It is the standard deviation divided by the dependent mean and usually expressed as a percent. The values of coefficient of variation for $Y1$ and $Y2$ models are 1.16 and 0.84, respectively, which are low enough to ensure significant models.

Effects of Oxidation Parameters on Textural Characteristics. Based on the results of ANOVA, all of the three oxidation parameters (acid concentration, temperature, and time) are significant variables for BET surface area. All have negative (antagonistic) effects on the response. F-values of these variables (Table 3) imply that oxidation time has the least effect, whereas the two others have much stronger effects (and quite similar) on BET surface area. However, according to ANOVA results, no interactions of factors are found to be significant. Figure 3 shows the selected three-dimensional (3D) response surfaces for BET surface area. In each plot, the third

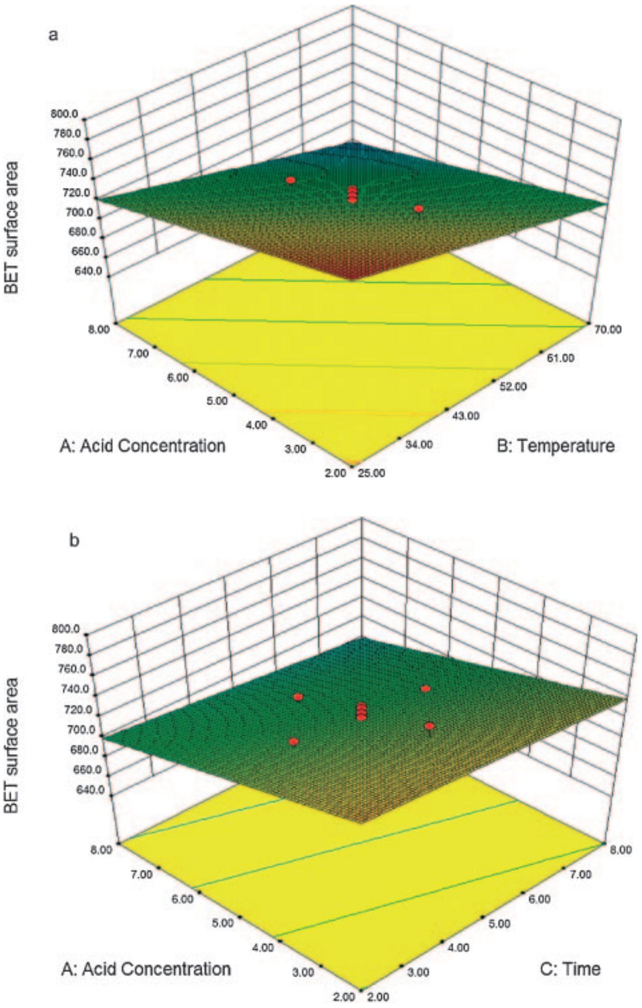

Figure 3. 3D response surface plot of BET surface area: a) effects of acid concentration and temperature; b) effects of acid concentration and time.

variable is fixed at zero level. It is apparent from Figure 3a that BET surface area decreases with increase in acid concentration and temperature so that the highest surface area is related to the minimum examined points (level -1) for both shown variables. By coupling this with what is shown in Figure 3b, it can be concluded graphically that BET surface area decrease with any increase in each of the variables. This fact has been already described by negative signs of the related terms in the adopted model. Linear change in BET surface area by changes in the variables, which is quantitatively indicated by the regression model equation, is visually sensible in Figures 3a and 3b. Considering the above, acid concentration, time, and temperature are regarded as oxidation severity parameters. The results obtained here state destructive effects of oxidation by nitric acid on textural characteristic of AC. It is widely reported that wet oxidation (oxidation by liquid oxidants such as nitric acid) results in decrease in surface area and pore volume.[7,21,33,34,37,47–54] These observations can be assigned to destruction of micropores, pore blockage by created oxygen groups or large molecules of humic material (which is produced by acidic treatment) and electrostatic repulsion of surface probe molecules (nitrogen).[16,21,28,40,55–61]

The effects of oxidation by nitric acid on different textural characteristics of the examined AC can be reviewed in Table 5. It may be observed from this table that the total pore volume (V_t) and the micropore volume ($V_{mic(DR)}$ and $V_{mic(t\text{-}plot)}$, in which “DR” and “t-plot” imply the methods of calculating V_{mic}) decrease with the increase in one or more of the oxidation severity parameters. $V_t - V_{mic(DR)}$, as an estimation of mesopore and macropore volume has been included in Table 5. It can be seen from the table that changes in textural characteristics follow almost the same trend.

However, it is noteworthy mentioning that despite the decrease in surface area and pore volume of AC by oxidation, sample analysis shows that the studied AC keeps its microporous structure after oxidation. Figure 4 shows typical nitrogen adsorption–desorption isotherms at 77 K for the parent and some of the selected oxidized samples. According to IUPAC classification, all the isotherms are type I that point to a dominant microporous structure. However, hysteresis loops show the presence of mesopores in the structure of all the samples.

Effects of Oxidation Parameters on Surface Chemistry. Study of AC Surface Chemistry Using TPD: Figure 5 shows typical TPD spectra for the parent and some oxidized samples. As it can be observed from the figure, the untreated AC (A1) has four obvious peaks at temperatures 70, 241, 682, and 852 °C. Oxidation by nitric acid increases the height of some peaks and creates new peaks and shoulders. The first peak (at 70 °C) exists for all oxidized samples at temperatures between 55–70 °C. It is probably related to physisorbed water. A shoulder around 160–180 °C and a peak around 410–420 °C are visible for all oxidized samples, compared with A1. To discuss creation of new oxygen groups or changes in existing ones, we overlaid TPD spectra of all the samples and recognized eight temperatures regions for peaks and shoulders for the examined group of samples as shown in Table 6.

Assignment of the evolution peaks of the composite TPD spectra to the associated oxygen groups cannot be done definitely. However, the second and third peaks are attributed to carboxylic and lactones, respectively.[9,16,17,29,38,47,50,52,62–64] Table 7 presents TPD assignment extracted from literature for different oxygen surface groups.

Considering the changes in the height of TPD peaks with changes in oxidation severity parameters, the area below the TPD curve can describe the density of the oxygen groups on the surface of the samples satisfactorily. This is why it is used as a measured parameter to characterize the surface chemistry of the samples quantitatively. It should be noted that the first peak, which is assigned to the physisorbed water,[24,64] has not been considered for calculation of Oxygen Index.

Evaluation of Effects of Oxidation on AC Surface Chemistry Using RSM: ANOVA results for response $Y2$ (Table 4) indicate that all of the three oxidation parameters significantly affect Oxygen Index. Moreover, three two-factor interactions, i.e., all possible two-factor interactions are found to be significant. All these terms have positive (synergistic) signs in the adopted model. In other words, all these terms have favorable influence on creation of oxygen groups on AC surface. Reviewing F-values of the model terms, which are shown in Table 4, indicate that oxidant concentration and temperature (with F-values of 800.58 and 806.15, respectively)

Table 5. Measured Characteristics of the Parent and Oxidized ACs

Sample Name	BET surface area ($Y1$) /m^2 g^{-1}	$S_{\text{mic(t-plot)}}$ /m^2 g^{-1}	V_{t} /m^3 g^{-1}	$V_{\text{mic(DR)}}$ /m^3 g^{-1}	$V_{\text{mic(t-plot)}}$ /m^3 g^{-1}	$V_{\text{t}} - V_{\text{mic(DR)}}$ /m^3 g^{-1}
A1	846.3	599.5	0.434	0.395	0.276	0.039
1	786.3	578.8	0.426	0.384	0.281	0.042
2	722.5	541.5	0.387	0.354	0.263	0.033
3	727.6	543.7	0.387	0.356	0.264	0.031
4	670.1	505.6	0.354	0.328	0.246	0.026
5	767.1	575.0	0.412	0.376	0.279	0.036
6	716.9	542.1	0.38	0.351	0.264	0.029
7	703.1	525.9	0.376	0.344	0.256	0.032
8	639.0	471.4	0.34	0.312	0.229	0.028
9	746.5	545.5	0.394	0.356	0.264	0.038
10	710.0	522.1	0.376	0.345	0.255	0.031
11	732.0	552.7	0.394	0.361	0.268	0.033
12	695.9	521.8	0.376	0.344	0.253	0.032
13	731.7	542.4	0.382	0.351	0.263	0.031
14	718.5	537.3	0.376	0.348	0.259	0.028
15	723.7	529.6	0.39	0.356	0.259	0.034
16	732.9	532.4	0.386	0.35	0.259	0.036
17	730.9	539.5	0.375	0.348	0.260	0.027
18	706.0	539.8	0.385	0.353	0.261	0.032
19	726.6	546.8	0.381	0.349	0.261	0.032
20	721.6	536.8	0.382	0.350	0.260	0.032

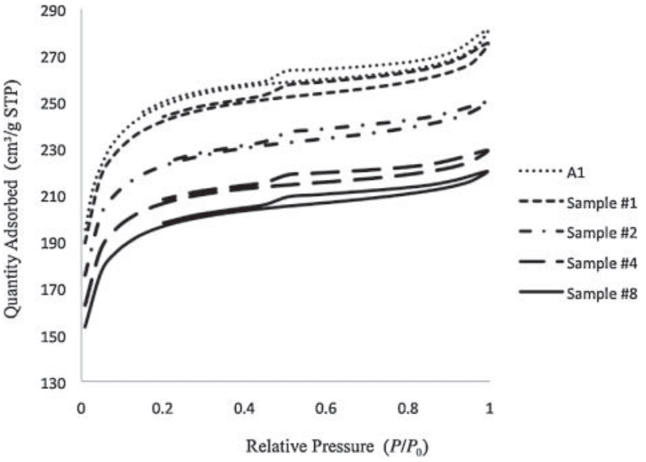

Figure 4. Typical nitrogen adsorption–desorption isotherms.

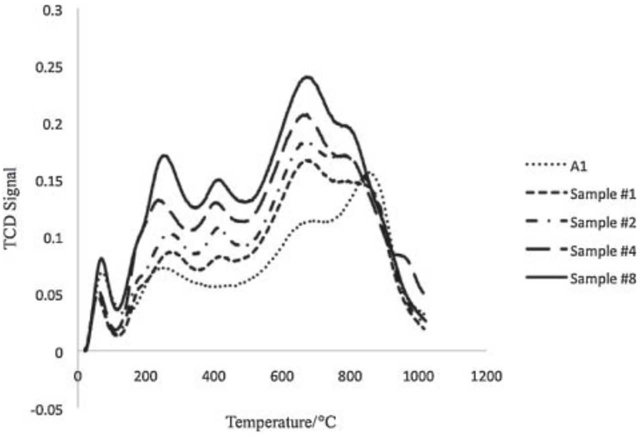

Figure 5. Typical TPD spectra of the selected samples.

Table 6. Temperature Regions of Peaks and Shoulders for the Parent and Oxidized Samples

Peaks	1	2	3	4	5	6	7	8
Temperature regions/°C	56–71	170–185	235–280	407–420	650–680	750–785	850–870	955–965

have the highest (and quite similar) effects on creation of oxygen groups. However, time effect is less dominant compared to concentration and temperature, but its effect is still considerable and higher than interactions effects. On the other hand, acid concentration–temperature and temperature–time interactions have moderate effects, whereas concentration–time is an interaction with the least effect on Oxygen Index response. Figure 6 shows the selected three-dimensional (3D) response surfaces for Oxygen Index. Each plot is shown at zero level of the third variable.

Figures 6a and 6b graphically indicate that density of oxygen groups generally increases with the increase in acid concentration, temperature, time, or any combination of them, so that the response of Oxygen Index can be maximized in the selected range of operating conditions by adopting all the variables at their highest level. The interpretation that is offered here based on regression model, F-value and 3D surface responses is as expected, because it agrees quite well with the published literature. Oxidation severity parameters that were considered as independent variables in the present work have been widely reported to be responsible for generation of different types of oxygen surface groups on AC. It is well known that nitric acid oxidation creates a large amount of carboxylic groups on AC surface.[10,11,34,38,48,66] Moreover, some

Table 7. TPD Assignment

Evolved gas	Oxygen groups	TPD temperature assignment/°C
CO_2	Carboxylic groups	200–500,[62][a)] 200–250,[9,38,63][b)] 350–400,[63][c)] 250,[9,38,64] 270,[52] 127–350,[47] 100–400,[9] 200–300,[17] 200–600,[16] <400[50]
	Lactones	370–670,[52] 627,[9,38] 650,[50] 350–400,[9,38,63] 190–650[9,17]
	Carboxylic anhydrides	370–670,[52] 600,[9,38] 627,[9,38,47,64] 350–400,[9,38,63] 400–577,[47] 440,[65] 350–657,[38] 550,[50] 800–900[17]
	Peroxide	550–600[63]
CO	Carboxylic anhydrides	370–670,[52] 400–577,[47] 440,[65] 350–400,[9] 600,[9] 627,[9] 550,[50] 400–450[63]
	Phenol	350–450,[62] 620,[52] 600–700,[9,17,38,47,63] 700[50]
	Carbonyl	450–700,[62] 810,[52] 800–900,[9,38,47,63] 700–980,[38] 500–980,[9] 800–980,[17] 850[50]
	Ether	350–450,[62] 700,[38] 800–900,[9] 700–980[9]
	Quinone	450–700,[62] 700–980,[9,38] 800–900,[9,38,63] 900–1027,[47] 900[17]
	Hydroquinone	600–700[63]
	Pyrone/Chromene	>1000[50,63]

a) Different acidities. b) Strongly acidic. c) Less acidic.

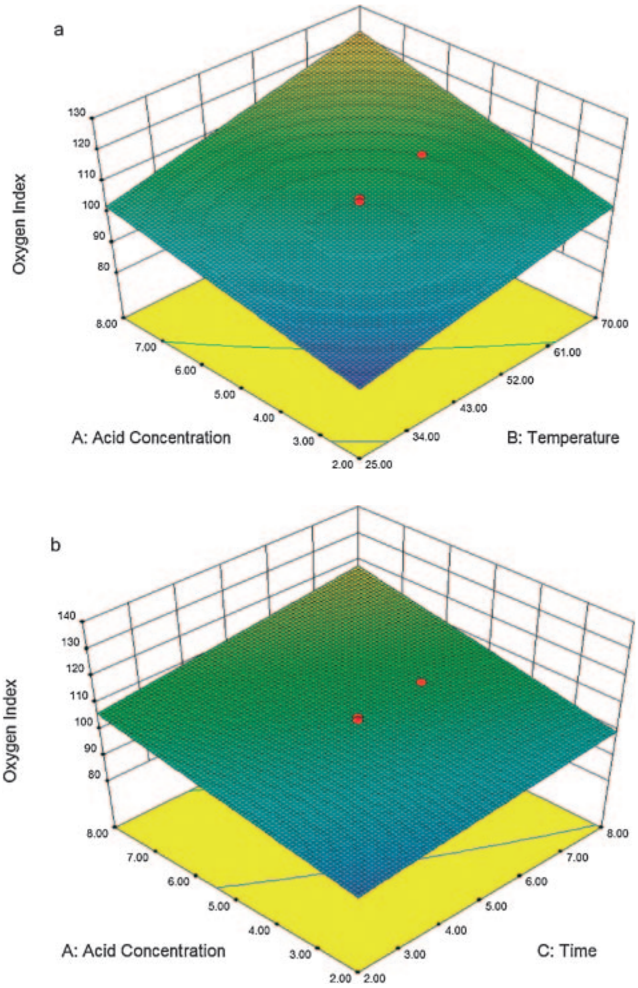

Figure 6. 3D response surface plot of Oxygen Index: a) effects of acid concentration and temperature; b) effects of acid concentration and time.

studies report creation of phenol and carboxylic groups on the surface on AC in higher orders.[40,41,67,68] However, it should be noted that Oxygen Index is an index of total oxygen groups, not exactly acidic surface groups. The effect of oxidation parameters on AC surface chemistry in terms of created oxygen groups have been studied.[59,69–71]

Oxidation Optimization. In application of AC as adsorbent (or catalyst), both textural properties and surface chemistry are generally important. AC surface chemistry is discussed from the view point of type and density of available surface groups. Research shows any modification in surface chemistry of AC usually causes changes in textural characteristics such as surface area and pore volume. As discussed in this paper, oxidation, which is performed to add oxygen surface groups to the AC structure, results in undesired changes in surface area and pore volume. In other words, tailoring the surface chemistry of AC with oxygen functionalities is carried out at the expense of losing surface area. Consequently, it is impossible to find conditions at which both BET surface area and Oxygen Index, which represent texture and surface chemistry of AC, are at their highest value at the same time. Therefore, it is rational to carry out a compromise between them.

In order to process optimization, some requirements for the factors and responses need to be set forth. For the purpose of this paper, both the responses are specified as "maximize," while all the factors were defined to be "in the range" in optimization module of Design Expert. The option of "include standard error models" was activated as well. This module defines a term called Desirability (that can range from zero to one) and determines optimum operating conditions to maximize Desirability. The results of optimization are usually demonstrated using contour plots. Each contour shows a constant value of the response as indicated on the contour and each point of the contour gives the operating conditions needed to reach that value of the response. In addition, the figures display a flag indicating the point of maximum Desirability. The operating conditions of the optimum point and the predicted values of each response are shown in the contour plots. Contour plots for the responses of BET surface area and Oxygen Index are represented in Figures 7a, 7b, and 7c.

As can be seen from Figure 7, optimum operating conditions are at acid concentration of 5.14 $\mathrm{mol\,L^{-1}}$, temperature of 48.39 °C and time of 5.22 h. At these conditions, it is predicted by the software of Design Expert to reach a BET surface area of

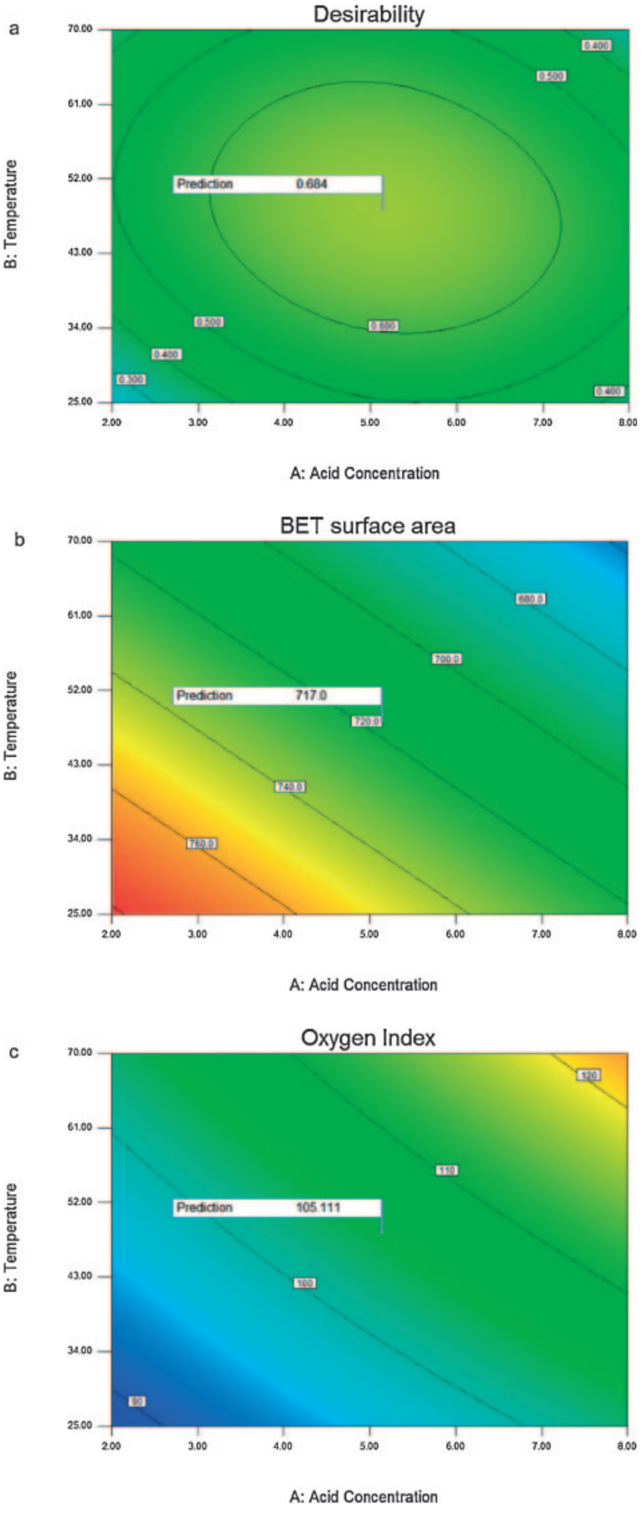

Figure 7. Contour plots for optimization: a) Desirability, b) BET surface area, and c) Oxygen Index.

717.0 and an Oxygen Index of 105.11, while a Desirability of 0.684 is predicted to be achieved. At the optimum operating conditions, the oxidation of AC was performed to test the validity of the models. The expermintal and predicted responses along with the error at optimum operating condition are shown in Table 8. It is apparent from the table that the obtained experimental results agree quite well with the predicted ones.

Table 8. Experimental and Predicted Value of BET Surface Area and Oxygen Index at Optimum Operating Conditions

Response	Experimental values	Predicted values	Error/%
BET surface area	721.2	717.0	0.59
Oxygen Index	103.9	105.11	−1.15

Conclusion

Oxidation of AC by nitric acid was explored to tailor its surface chemistry for further modification. A CCD was carried out to study the influences of three oxidation severity parameters including acid concentration, temperature, and time of oxidation on BET surface area (a measurement of textural characteristics) and Oxygen Index (an index indicating density of oxygen surface groups) of AC. A linear model was developed for BET surface area, whereas Oxygen Index results were found to be fitted by a 2FI model. The statistical analysis demonstrated that BET surface area and Oxygen Index are strongly affected by acid concentration and temperature, whereas the effect of time is less, but still considerable, for both responses. It was also found that interactions of parameters have moderate effects on Oxygen Index, but they are not significant in the case BET surface area response. Using optimization module, optimum operating conditions were achieved at acid concentration of 5.14 mol L^{-1}, temperature of 48.39 °C and time of 5.22 h. Experimental results at optimum conditions presented a good agreement with the predicted value. Since textural characteristics such as surface area, total pore volume, and micropore volume were negatively affected even at a mild severity, it can be concluded that the utilized AC has already a developed structure, so more oxidation causes a negative effect on the textural characteristic. On the other hand, TPD spectra obviously indicate creation of much oxygen functional groups, especially the acidic ones. At the most severe conditions experienced in this study, a decrease of about 25% in surface area and an increase of 76% in oxygen functional groups (based on Oxygen Index) were noted.

It is concluded from the results that oxidation affects the surface chemistry of AC more serious than the texture. Moreover, the results suggest that by adjusting the oxidation parameters, the amount of created oxygen groups and the degree of oxidation can be easily controlled. Therefore, one can tailor the surface of this AC efficiently with oxygen functional group by nitric acid for a minor effect on its texture.

Financial support by Ministry of Science, Technology and innovations of science fund "No. 13-02-03-3070" and University of Malaya are gratefully acknowledged.

References

1 W. M. A. W. Daud, A. H. Houshamnd, *J. Nat. Gas Chem.* **2010**, *19*, 267.

2 T. J. Bandosz, C. O. Ania, *Interface Sci. Technol.* **2006**, *7*, 159.

3 T. C. Drage, A. Arenillas, K. M. Smith, C. Pevida, S. Piippo, C. E. Snape, *Fuel* **2007**, *86*, 22.

4 H. T. Gomes, B. F. Machado, A. Ribeiro, I. Moreira, M. Rosário, A. M. T. Silva, J. L. Figueiredo, J. L. Faria, *J. Hazard. Mater.* **2008**, *159*, 420.

5 C. Y. Yin, M. K. Aroua, W. M. A. W. Daud, *Sep. Purif. Technol.* **2007**, *52*, 403.

6 J. Jaramillo, V. Gómez-Serrano, P. M. Álvarez, *J. Hazard. Mater.* **2009**, *161*, 670.

7 A. H. El-Sheikh, *Talanta* **2008**, *75*, 127.

8 J. de Celis, N. E. Amadeo, A. L. Cukierman, *J. Hazard. Mater.* **2009**, *161*, 217.

9 H.-H. Tseng, M.-Y. Wey, *Chemosphere* **2006**, *62*, 756.

10 Z. H. Zhu, L. R. Radovic, G. Q. Lu, *Carbon* **2000**, *38*, 451.

11 A. E. Aksoylu, M. Madalena, A. Freitas, M. F. R. Pereira, J. L. Figueiredo, *Carbon* **2001**, *39*, 175.

12 Y. Xue, Y. Guo, Z. Zhang, Y. Guo, Y. Wang, G. Lu, *Appl. Surf. Sci.* **2008**, *255*, 2591.

13 A. Zhou, X. Ma, C. Song, *Appl. Catal., B* **2009**, *87*, 190.

14 H. Cui, S. Q. Turn, M. A. Reese, *Catal. Today* **2009**, *139*, 274.

15 R. V. R. A. Rios, J. Silvestre-Albero, A. Sepúlveda-Escribano, F. Rodríguez-Reinoso, *Colloids Surf., A* **2007**, *300*, 180.

16 Y. El-Sayed, T. J. Bandosz, *J. Colloid Interface Sci.* **2001**, *242*, 44.

17 C. Aguilar, R. García, G. Soto-Garrido, R. Arriagada, *Appl. Catal., B* **2003**, *46*, 229.

18 A. Houshmand, W. M. A. W. Daud, M. S. Shafeeyan, *Sep. Sci. Technol.* **2011**, *46*, 1098.

19 A. R. Silva, V. Budarin, J. H. Clark, C. Freire, B. de Castro, *Carbon* **2007**, *45*, 1951.

20 H. Tamai, K. Shiraki, T. Shiono, H. Yasuda, *J. Colloid Interface Sci.* **2006**, *295*, 299.

21 H. F. Gorgulho, J. P. Mesquita, F. Gonçalves, M. F. R. Pereira, J. L. Figueiredo, *Carbon* **2008**, *46*, 1544.

22 Y. Matsuo, Y. Nishino, T. Fukutsuka, Y. Sugie, *Carbon* **2008**, *46*, 1162.

23 Y. Matsuo, Y. Nishino, T. Fukutsuka, Y. Sugie, *Carbon* **2007**, *45*, 1384.

24 N. Toumi, I. Bonnamour, J.-P. Joly, G. Finqueneisel, L. Retailleau, R. Kalfat, R. Lamartine, *Mater. Sci. Eng., C* **2006**, *26*, 490.

25 A. R. Silva, M. Martins, M. M. A. Freitas, A. Valente, C. Freire, B. de Castro, J. L. Figueiredo, *Microporous Mesoporous Mater.* **2002**, *55*, 275.

26 C. Pevida, M. G. Plaza, A. Arias, J. Fermoso, F. Rubiera, J. J. Pis, *Appl. Surf. Sci.* **2008**, *254*, 7165.

27 C. L. Mangun, K. R. Benak, J. Economy, K. L. Foster, *Carbon* **2001**, *39*, 1809.

28 R. J. J. Jansen, H. van Bekkum, *Carbon* **1994**, *32*, 1507.

29 M. S. Shafeeyan, W. M. A. W. Daud, A. Houshmand, A. Shamiri, *J. Anal. Appl. Pyrolysis* **2010**, *89*, 143.

30 V. Gómez-Serrano, P. M. Álvarez, J. Jaramillo, F. J. Beltrán, *Carbon* **2002**, *40*, 513.

31 H. P. Boehm, *Carbon* **2002**, *40*, 145.

32 A. Derylo-Marczewska, A. Swiatkowski, S. Biniak, M. Walczyk, *Colloids Surf., A* **2008**, *327*, 1.

33 C. O. Ania, J. B. Parra, J. J. Pis, *Fuel Process. Technol.* **2002**, *79*, 265.

34 I. I. Salame, T. J. Bandosz, *J. Colloid Interface Sci.* **1999**, *210*, 367.

35 Y. El-Sayed, T. J. Bandosz, *J. Colloid Interface Sci.* **2004**, *273*, 64.

36 M. Domingo-García, F. J. López-Garzón, M. Pérez-Mendoza, *J. Colloid Interface Sci.* **2000**, *222*, 233.

37 F. Julien, M. Baudu, M. Mazet, *Water Res.* **1998**, *32*, 3414.

38 J. L. Figueiredo, M. F. R. Pereira, M. M. A. Freitas, J. J. M. Órfão, *Carbon* **1999**, *37*, 1379.

39 I. I. Salame, T. J. Bandosz, *J. Colloid Interface Sci.* **2001**, *240*, 252.

40 V. Strelko, Jr., D. J. Malik, M. Streat, *Carbon* **2002**, *40*, 95.

41 C. U. Pittman, Jr., G.-R. He, B. Wu, S. D. Gardner, *Carbon* **1997**, *35*, 317.

42 Q. Jia, A. C. Lua, *J. Anal. Appl. Pyrolysis* **2008**, *83*, 175.

43 J. Guo, A. C. Lua, *Mater. Lett.* **2002**, *55*, 334.

44 I. Arslan-Alaton, G. Tureli, T. Olmez-Hanci, *J. Photochem. Photobiol., A* **2009**, *202*, 142.

45 R. Azargohar, A. K. Dalai, *Microporous Mesoporous Mater.* **2005**, *85*, 219.

46 B. H. Hameed, I. A. W. Tan, A. L. Ahmad, *J. Hazard. Mater.* **2008**, *158*, 324.

47 L. J. Lemus-Yegres, I. Such-Basáñez, M. C. Román-Martínez, C. Salinas-Martínez de Lecea, *Appl. Catal., A* **2007**, *331*, 26.

48 I. I. Salame, T. J. Bandosz, *J. Colloid Interface Sci.* **2003**, *264*, 307.

49 A. L. Chaffee, G. P. Knowles, Z. Liang, J. Zhang, P. Xiao, P. A. Webley, *Int. J. Greenhouse Gas Control* **2007**, *1*, 11.

50 M. F. R. Pereira, S. F. Soares, J. J. M. Órfão, J. L. Figueiredo, *Carbon* **2003**, *41*, 811.

51 M. A. Álvarez-Merino, V. López-Ramón, C. Moreno-Castilla, *J. Colloid Interface Sci.* **2005**, *288*, 335.

52 V. Z. Radkevich, T. L. Senko, K. Wilson, L. M. Grishenko, A. N. Zaderko, V. Y. Diyuk, *Appl. Catal., A* **2008**, *335*, 241.

53 S. Tanada, N. Kawasaki, T. Nakamura, M. Araki, M. Isomura, *J. Colloid Interface Sci.* **1999**, *214*, 106.

54 A. Aburub, D. E. Wurster, *J. Colloid Interface Sci.* **2006**, *296*, 79.

55 P. M. Álvarez, J. F. García-Araya, F. J. Beltrán, F. J. Masa, F. Medina, *J. Colloid Interface Sci.* **2005**, *283*, 503.

56 A.-N. A. El-Hendawy, *Carbon* **2003**, *41*, 713.

57 G. S. Szymański, T. Grzybek, H. Papp, *Catal. Today* **2004**, *90*, 51.

58 Y. H. Li, C. W. Lee, B. K. Gullet, *Fuel* **2003**, *82*, 451.

59 C. Moreno-Castilla, F. Carrasco-Marín, A. Mueden, *Carbon* **1997**, *35*, 1619.

60 V. Strelko, Jr., D. J. Malik, *J. Colloid Interface Sci.* **2002**, *250*, 213.

61 M. M. Maroto-Valer, I. Dranca, T. Lupascu, R. Nastas, *Carbon* **2004**, *42*, 2655.

62 G. G. Stavropoulos, P. Samaras, G. P. Sakellaropoulos, *J. Hazard. Mater.* **2008**, *151*, 414.

63 U. Zielke, K. J. Hüttinger, W. P. Hoffman, *Carbon* **1996**, *34*, 983.

64 Y. Otake, R. G. Jenkins, *Carbon* **1993**, *31*, 109.

65 S. Biniak, G. Szymański, J. Siedlewski, A. Świątkowski, *Carbon* **1997**, *35*, 1799.

66 I. F. Silva, J. Vital, A. M. Ramos, H. Valente, A. M. Botelho do Rego, M. J. Reis, *Carbon* **1998**, *36*, 1159.

67 C. U. Pittman, Jr., G.-R. He, B. Wu, S. D. Gardner, *Carbon* **1997**, *35*, 333.

68 C. U. Pittman, Jr., Z. Wu, W. Jiang, G.-R. He, B. Wu, W. Li, S. D. Gardner, *Carbon* **1997**, *35*, 929.

69 S. S. Barton, M. J. B. Evans, E. Halliop, J. A. F. MacDonald, *Carbon* **1997**, *35*, 1361.

70 M. Takaoka, H. Yokokawa, N. Takeda, *Appl. Catal., B* **2007**, *74*, 179.

71 M. J. Lázaro, L. Calvillo, E. G. Bordejé, R. Moliner, R. Juan, C. R. Ruiz, *Microporous Mesoporous Mater.* **2007**, *103*, 158.